[^{11}C]glyburide PET imaging for quantitative determination of the importance of Organic Anion-Transporting Polypeptide transporter function in the human liver and whole-body

Solène Marie, Louise Breuil, Zacharias Chalampalakis, Laurent Becquemont, Céline Verstuyft, Anne-Lise Lecoq, Fabien Caillé, Philippe Gervais, Vincent Lebon, Claude Comtat, et al.

Biomedicine & Pharmacotherapy 156 (2022) 113994

Contents lists available at ScienceDirect

Biomedicine & Pharmacotherapy

journal homepage: www.elsevier.com/locate/biopha

[^{11}C]glyburide PET imaging for quantitative determination of the importance of Organic Anion-Transporting Polypeptide transporter function in the human liver and whole-body

Solène Marie [a,b,c,1], Louise Breuil [a,2], Zacharias Chalampalakis [a,3], Laurent Becquemont [d,f,4], Céline Verstuyft [e,f,5], Anne-Lise Lecoq [d,6], Fabien Caillé [a,7], Philippe Gervais [a,8], Vincent Lebon [a,9], Claude Comtat [a,10], Michel Bottlaender [a,11], Nicolas Tournier [a,*,12]

[a] Université Paris-Saclay, CEA, Inserm, CNRS, BioMaps, Service Hospitalier Frédéric Joliot, 4 place du Général Leclerc, 91401 Orsay, France
[b] Département de Pharmacie Clinique, Faculté de Pharmacie, Université Paris-Saclay, 92296 Châtenay-Malabry, France
[c] AP-HP, Université Paris-Saclay, Hôpital Bicêtre, Pharmacie Clinique, 94270 Le Kremlin Bicêtre, France
[d] AP-HP, Université Paris-Saclay, Hôpital Bicêtre, Centre de Recherche Clinique, 94270 Le Kremlin Bicêtre, France
[e] AP-HP, Université Paris-Saclay, Hôpital Bicêtre, Service de génétique Moléculaire, Pharmacogénétique et Hormonologie, 94270 Le Kremlin Bicêtre, France
[f] CESP, MOODS Team, INSERM UMR 1018, Faculté de Médecine, Univ Paris-Saclay, Le Kremlin Bicêtre F-94275, France

ARTICLE INFO

Keywords:
[^{11}C]glyburide
Hepatocyte
Liver
PET
Pharmacokinetics

ABSTRACT

Organic Anion-Transporting Polypeptides (OATPs) are known to control the liver uptake of many drugs. Non-hepatic expression of OATPs has been reported although functional importance for whole-body pharmacokinetics (WBPK) remains unknown. Glyburide is a well described substrate of several hepatic and non-hepatic OATPs. Dynamic whole-body positron emission tomography (DWB-PET) with [^{11}C]glyburide was performed in humans for determination of the importance of OATPs for liver uptake and WBPK. Seven healthy male subjects (24.7 ± 3.2 years) underwent [^{11}C]glyburide PET scan with concomitant blood sampling. All subjects underwent

Abbreviations: ABC, ATP-binding cassette; AUC, area under the curve; AUCR, ratio of AUC_{tissue} to AUC_{blood}; BBB, blood-brain barrier; BCRP, breast cancer resistance protein; $C_{blood,t}$, blood concentration at time t; $C_{liver,t}$, liver concentration at time t; COVID-19, coronavirus disease-19; CT, computed tomography; DDI, drug-drug interaction; DILI, drug-induced liver injury; DWB, dynamic whole-body; f_b, fraction bound to plasma protein; HPLC, high-performance liquid chromatography; IDIF, image-derived input function; k_{uptake}, uptake transfer constant; MR, magnetic resonance; MRAC, MR based PET attenuation correction; OATP, organic anion-transporting polypeptide; OAT, organic anion transporter; OCT, organic cation transporter; P-gp, P-glycoprotein; PET, positron emission tomography; PK, pharmacokinetics; SD, standard deviation; SUV, standardized uptake value; SUV_{max}, maximum standardized uptake value; SLC, solute carrier; SUR1, type 1 sulfonylurea receptors; TAC, time–activity curve; UV, ultraviolet; V_E, initial distribution volume in the liver at time 0; VOI, volume of interest; WBPK, whole-body pharmacokinetics.

* Correspondence to: CEA/SHFJ, 4 place du Général Leclerc, 91400 Orsay, France.
E-mail addresses: solene.marie@aphp.fr (S. Marie), louise.breuil@universite-paris-saclay.fr (L. Breuil), zacharias.chalampalakis@universite-paris-saclay.fr (Z. Chalampalakis), laurent.becquemont@aphp.fr (L. Becquemont), celine.verstuyft@aphp.fr (C. Verstuyft), anne-lise.lecoq@aphp.fr (A.-L. Lecoq), fabien.caille@cea.fr (F. Caillé), philippe.gervais@cea.fr (P. Gervais), vincent.lebon@universite-paris-saclay.fr (V. Lebon), claude.comtat@universite-paris-saclay.fr (C. Comtat), michel.bottlaender@universite-paris-saclay.fr (M. Bottlaender), nicolas.tournier@cea.fr (N. Tournier).
[1] **ORCID:** 0000-0001-5247-4871.
[2] **ORCID:** 0000-0003-2050-7469.
[3] **ORCID:** 0000-0003-3390-6979.
[4] **ORCID:** 0000-0003-3477-8956.
[5] **ORCID:** 0000-0002-8534-224X.
[6] **ORCID:** 0000-0002-8630-961X.
[7] **ORCID:** 0000-0003-0088-7337.
[8] **ORCID:** 0000-0003-2172-879X.
[9] **ORCID:** 0000-0003-2992-8710.
[10] **ORCID:** 0000-0003-4691-7001.
[11] **ORCID:** 0000-0002-2890-3653.
[12] **ORCID:** 0000-0002-0755-2030.

https://doi.org/10.1016/j.biopha.2022.113994
Received 3 September 2022; Received in revised form 7 November 2022; Accepted 7 November 2022
Available online 9 November 2022

Positron emission tomography
Transporters

baseline [^{11}C]glyburide PET scan. Five subjects underwent a subsequent [^{11}C]glyburide PET scan after infusion of the potent OATP inhibitor rifampicin (9 mg/kg i.v.). The transfer constant (k_{uptake}) of [^{11}C]glyburide from blood to the liver was estimated using the integration plot method. The tissue exposure of [^{11}C]glyburide was described by the area under the time-activity curve (AUC) and corresponding tissue/blood ratio (AUCR). [^{11}C]glyburide was barely metabolized in both the baseline and rifampicin conditions. Parent (unmetabolized) [^{11}C]glyburide accounted for > 90 % of the plasma radioactivity. Excellent correlation was found between radioactive counting in arterial blood samples and in the image-derived input function, in both the baseline and rifampicin conditions (R^2 = 97.9 %, $p < 0.01$). [^{11}C]glyburide predominantly accumulated in the liver. Rifampicin decreased liver k_{uptake} by 77.3 ± 7.3 %, which increased exposure in blood, kidneys, spleen, myocardium and brain ($p < 0.05$). No significant change in AUCR was observed except in the liver ($p < 0.01$). [^{11}C]glyburide benefits from metabolic stability and high sensitivity to OATP inhibition which enables quantitative determination of OATP function. DWB-PET suggests negligible role for non-hepatic OATPs in controlling the tissue distribution of [^{11}C]glyburide.

1. Introduction

It is often hypothesized that passive diffusion is the main mechanism mediating drug diffusion from circulation to organs. However, identification of membrane transporters at the blood-tissue interface suggests that delivery of drugs to tissues may be controlled by carrier-mediated processes [1–4]. Influx transporters of the Solute Carrier (SLC) superfamily enable the blood-to-tissue transfer of several endogenous and exogenous compounds. Transporters of the Organic Anion-Transporting Polypeptide (OATP) family are well known to mediate the hepatic uptake of many drugs [5]. Liver OATPs include OATP1B1, OATP1B3, and OATP2B1. OATP1B1/1B3 are assumed to be liver-specific although non-hepatic expression of OATP1B3 has been reported [6]. Expression of OATP2B1 is predominant in the liver but was also detected in non-clearance organs including human myocardium, blood-brain barrier (BBB), epithelial lung cells, ovary, mammary duct, and muscles. Other non-hepatic OATPs have been reported, including OATP1A2, whose expression has been detected in brain, liver, lung, kidney, and testis [7]. The importance for non-hepatic OATPs in controlling drug delivery to these potential target/vulnerable tissues relative to hepatic OATP function remains to be assessed *in vivo* [8].

So far, pharmacokinetic (PK) studies are mainly based on the time-concentration profile of drugs in plasma and body fluids [9]. This approach is commonly performed to investigate pharmacokinetic drug-drug interactions (DDIs) involving transporters including OATPs [3]. However, from a perspective of drug efficacy or toxicity, it is the tissue concentration rather than plasma concentration that is the most relevant. Efforts are currently being made to consider PK as a global and whole-body approach (WBPK) [10,11]. In this framework, dynamic whole-body (DWB) positron emission tomography (PET) imaging using radiolabeled analogs of drugs is emerging as an innovative method to unveil the delivery of drugs in the whole-body [12,13] and explore molecular mechanisms controlling the WBPK of drugs in animals and humans [14].

Efforts have been made to develop dedicated PET probes to investigate the impact of efflux transporters of the ATP-binding cassette (ABC) family on drug delivery to selected organs such as the brain [15, 16] or the lungs [17]. The role of SLC transporters did not receive as much attention although their importance for WBPK remains unclear [2, 18]. Several probes have been proposed for quantitative PET imaging of liver OATP function [19]. So far, clinically validated PET probes used in humans include (15 *R*)-[^{11}C]TIC-Me, [^{11}C]dehydropravastatin, [^{11}C]telmisartan, [^{11}C]rosuvastatin, and [^{11}C]erlotinib [20–24]. The substrate profile of these probes corresponds to hepatic OATPs (OATP1B1/1B3 and/or OATP2B1) and imaging acquisitions consisted of dynamic acquisitions focused on the liver. A major limitation of current probes is the formation of radiometabolites causing the PET signal associated with radiometabolites in tissues to be indistinguishable from that associated with the parent (unmetabolized) radioligand. Metabolic stability is therefore essential for correct interpretation of PET data, especially in the liver which is the main site for drug metabolism [14]. Another important feature of PET probes for influx transporters is the sensitivity to detect changes in transporter function [14]. Sensitivity of investigated substrate probes to inhibition is usually estimated by the magnitude of the decreased liver uptake precipitated by inhibition/depletion of transporter function. This can be easily achieved for liver OATPs in humans using a single dose of rifampicin, a safe and potent OATP inhibitor [3]. Finally, the liver uptake of an ideal PET probe for OATPs should be negligible when transporters are inhibited, thus ensuring the specificity of the carrier-mediated transport over passive diffusion or other transporter systems.

Glyburide (5-chloro-N-[2-[4-(cyclohexylcarbamoylsulfamoyl) phenyl]ethyl]-2-methoxybenzamide, *a.k.a* glibenclamide) is a hypoglycemic agent commonly used in the treatment of noninsulin-dependent diabetes. The type 1 surfonylurea receptors (SUR1) subunits are the binding site of glyburide which induces insulin secretion by pancreatic cells through inhibitory effect on the K_{ATP} channel [25]. Recent *in vitro* and simulation studies suggest that the carrier-mediated uptake of glyburide by the liver is predominantly mediated by OATP1B1 [26]. This is consistent with clinical studies showing significant DDIs with decreased plasma clearance of glyburide following administration of rifampicin in humans [27,28]. However, previous *in vitro* studies suggest that glyburide may also be substrate for non-hepatic OATP2B1 and OATP1A2, which may impact WPBK [29,30].

Isotopic radiolabeling of glyburide with carbon-11 ([^{11}C]glyburide) is feasible [31]. [^{11}C]glyburide PET imaging was therefore evaluated in healthy volunteers as a probe for OATP function. An optimized DWB-PET acquisition protocol using a PET-MR (magnetic resonance) system was performed to simultaneously compare [^{11}C]glyburide distribution in the liver and other organs in order to assess the importance of OATP-mediated transport on the WBPK of glyburide in humans.

2. Material and methods

2.1. Radiosynthesis of [^{11}C]glyburide

[^{11}C]glyburide was synthesized using a previously described automated two-step method [31]. Detailed information are provided as Supplementary data.

2.2. Subjects and study design

The study protocol was approved by an Ethic Committee (CPP IDF5: 17041) and the experiments were conducted with respect of the Declaration of Helsinki. All subjects had a first medical examination where the inclusion criteria were checked by the clinical investigator. A written informed consent was signed after the subjects received the information about the study.

Eleven healthy male volunteers (< 30 years-old) were included in the study. Four of them did not participate to imaging sessions due to technical issues regarding radiosynthesis or the PET-MR system. Seven subjects (24.7 ± 3.2 years-old, body weight was 75 ± 10 kg)

participated to two subsequent imaging sessions which took place during a single day to avoid inter-day variability. An intravenous (i.v.) bolus of [^{11}C]glyburide was first injected. After 3 h decay, total PET signal represented < 0.22 % of injected radioactivity due to the very short radioactive half-life of carbon-11 (20.4 min). The second i.v. bolus of [^{11}C]glyburide was therefore injected at least 3 h later, immediately after infusion of rifampicin (9 mg/kg diluted in glucose 5 % perfused, within 45 min of [^{11}C]glyburide injection, Rifadin®, Sanofi-Aventis, Gentilly, France). All volunteers received the first injection of [^{11}C]glyburide (147 ± 63 MBq i.v.). Five of them received the second injection of [^{11}C]glyburide (161 ± 69 MBq i.v.) after infusion of rifampicin. The mean specific radioactivity at the time of injection was 7988 ± 4250 MBq/μmol. The pharmacokinetic half-life of i.v injected glyburide (1 mg) in human plasma is ~ 1.5 h [32]. Injected mass of glyburide associated with the first injection of [^{11}C]glyburide was probably not fully eliminated from the body at the time of the second injection. However, microdoses of glyburide (11.2 ± 5.8 μg) injected for PET imaging were very low compared with pharmacological dose (1.25–5 mg). Cumulative saturation of carrier-mediated transport is therefore very unlikely.

2.3. PET imaging

Whole-body dynamic acquisitions were performed using a SIGNA® PET/MR scanner (GE Healthcare, Waukesha, WI, USA). The three first subjects had a catheter inserted in one arm for arterial blood sampling and a venous catheter in the other arm for [^{11}C]glyburide injection. Due to the COVID-19 pandemic, access to anesthesiologist staff for insertion of the arterial catheter was no longer possible and a venous catheter was inserted instead for subsequent subjects to estimate the proportion of radiometabolites. The subjects were positioned on the patient bed and MR localization acquisitions were performed. A first blood sample was collected before [^{11}C]glyburide injection for determination of the binding to plasma proteins. PET acquisition began with the injection of [^{11}C]glyburide (1 min bolus). The first 3-minute dynamic mono-bed acquisition was positioned on the abdomen (16 frames of 10 s), to capture uptake in the liver and some abdominal organs including spleen, pancreas, kidneys, and myocardium. This was immediately followed by repeated multi-bed whole-body acquisitions performed over the next 27 min (5 bed positions, 11 frames of 2.5 min). Arterial blood samples were collected every 25 s in the first 4 min and at 5, 7, 10, 15, 20, and 30 min post-injection. Venous blood samples were collected at 1, 3, 5, 7, 10, 15, 20, and 30 min post-injection.

2.4. PET data analysis

PET images were reconstructed using a 3D-iterative reconstruction algorithm, including resolution modeling and time-of-flight. Data were corrected for radioactive decay, attenuation, and random and scattered coincidences. Attenuation correction was based on a 2-point Dixon MR sequence (MRAC). Volumes of interest (VOIs) were delineated for tissues (liver, kidneys, spleen, myocardium, pancreas, brain, testis, muscle, and eyes) which were delineated from PET and/or co-registered MRAC images using the PMOD® software (version 3.9, PMOD Technologies LLC, Zurich, Switzerland). An additional VOI was delineated on a multi-bed volume which includes the left ventricle and the aorta to derive an image-derived input function (IDIF). Time–activity curves (TACs) were generated by calculating the mean radioactivity in these VOI (kBq/cc). Standardized uptake values (SUV) were also generated by correcting the radioactivity in the VOI for injected dose and body weight. Areas under the TACs (AUC, expressed in SUV.min) were calculated from 0 to 30 min for each TAC to describe tissue exposure.

The transfer constant (k_{uptake}) of [^{11}C]glyburide from blood to the liver was estimated using the integration plot method [24,33] from 5 to 30 min after [^{11}C]glyburide injection using the equation $\frac{C_{liver,t}}{C_{blood,t}} = k_{uptake} \times \left(\frac{AUC_{blood,0-t}}{C_{blood,t}}\right) + V_E$, where $C_{liver,t}$ and $C_{blood,t}$ represent the concentrations of [^{11}C]glyburide in the liver and blood (IDIF) respectively at time t. $AUC_{blood,0-t}$ represents the area under the IDIF TAC from time 0 to t. k_{uptake} corresponds to the slope of the linear regression plot. V_E represents the initial distribution volume in the liver at time 0.

2.5. Plasma analysis

[^{11}C]glyburide plasma concentrations were estimated from blood samples by counting whole-blood (100 μL) and plasma (200 μL) with a gamma counter (Cobra®, Packard, Meriden, CT, USA). Plasma samples obtained at 5, 10, 15, and 30 min were deproteinized with acetonitrile and injected into an UV/radioactive-HPLC system (HPLC Waters e2965 with a Waters 2489 UV/vis detector, Guyancourt, France and FlowStar^2 Detector for Radio HPLC, Berthold, France). [^{11}C]glyburide was separated from its radiometabolites using a C18 semipreparative (10 × 250 mm, 10 μm) Atlantis® column (Waters, Guyancourt, France). The mobile phase consisted of 10 mM ammonium acetate in purified water (A) and acetonitrile (B). The gradient elution of B from 20 % at 0 min to 90 % at 12 min was applied to the column.

The [^{11}C]glyburide fraction bound to plasma protein (f_b) with and without rifampicin infusion was estimated on the first sample (obtained before injection of [^{11}C]glyburide). Plasma sample was added ~ 4 MBq of [^{11}C]glyburide and f_b was determined as previously described using a validated ultrafiltration method (MPS Micropartition Microcon®-YM-10 membrane, Millipore, Molsheim, France) [34].

2.6. Data and statistical analysis

Data were calculated as the mean ± SD (standard deviation). Linear regression was used to test the correlation between activity in arterial blood samples and IDIF. Paired *t*-test was used to identify differences before and after rifampicin-treatment on [^{11}C]glyburide kinetics ($p < 0.05$). Statistical analysis was performed using GraphPad Prism® software (version 8.4, San Diego, CA, USA).

3. Results

3.1. [^{11}C]glyburide blood data

[^{11}C]glyburide was barely metabolized in both the baseline and rifampicin conditions (Supplemental Fig. 1). Parent (unmetabolized) [^{11}C]glyburide in either arterial (n = 6) or venous (n = 4) plasma samples accounted for more than 90 % of the plasma radioactivity over PET acquisition (Fig. 1A). A small proportion of radiometabolites could be detected in baseline condition at each time point (maximum 6.8 ± 3.6 % at 10 min). In the presence of rifampicin, radiometabolites could only be detected at 5 min after injection (6.0 ± 2.4 %) but not at later time points. It was therefore decided not to correct the arterial input function from radiometabolites given their limited impact on PET quantification.

[^{11}C]glyburide is known to be highly bound to plasmatic proteins [35]. Plasma protein binding was 99.45 ± 0.01 % in baseline experiments (n = 7). Rifampicin did not impact binding to plasma proteins which was 99.33 ± 0.01 % in rifampicin-treated subjects who underwent arterial blood sampling (n = 3). Rifampicin did not impact the plasma/whole-blood ratio which was 1.65 ± 0.17 in baseline and 1.62 ± 0.14 in rifampicin-treated subjects at the end of PET acquisition (n = 4, p > 0.05).

Correlation of [^{11}C]glyburide concentrations measured from whole-blood samples and IDIF obtained in the 3 subjects who underwent arterial blood sampling is presented in Fig. 1B. Linear regression was calculated for both baseline and rifampicin situations and confirmed excellent correlation (R^2 = 98.6 % in baseline condition, R^2 = 96.8 % after treatment by rifampicin and R^2 = 97.9 % with both combined). This enabled the use of IDIF for kinetic modeling of [^{11}C]glyburide PET data, with no need for arterial catheterization.

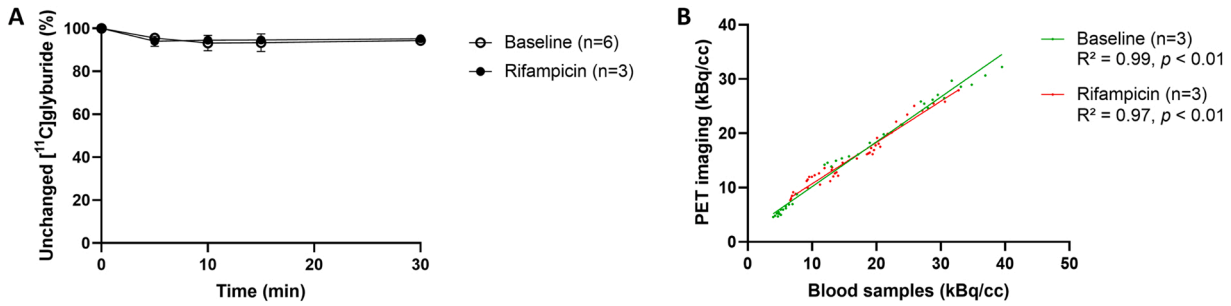

Fig. 1. [^{11}C] glyburide metabolism in healthy volunteers in absence and presence of rifampicin (9 mg/kg i.v.) (A). Correlation of whole-blood concentrations of ^{11}C] glyburide (kBq/cc) measured from gamma-counting of blood samples with PET quantification (image derived input function) obtained in the baseline and the rifampicin-treated groups (B). Metabolism data are presented as mean percentages ± SD of unchanged [^{11}C]glyburide in plasma *vs* time after i.v. injection of [^{11}C]glyburide in baseline conditions and after rifampicin infusion.

3.2. [^{11}C]glyburide PET data

Representative PET images of the whole-body distribution of [^{11}C] glyburide with and without rifampicin are shown in Fig. 2. Under baseline conditions, [^{11}C]glyburide showed a slow but predominant uptake by the liver (SUV_{max} = 18.6 ± 3.9 at 30 min, Fig. 3) but also substantial distribution to the kidneys. Lower uptake by the myocardium and spleen was observed (Fig. 2). Uptake by other tissues was extremely low and associated with high variability, probably due to the poor signal counting. Strikingly, radioactivity was obvious in the circulation, reflecting high retention of [^{11}C]glyburide in the plasma, probably due to high binding to plasmatic proteins and/or limited diffusion of [^{11}C]glyburide from blood to most tissues.

Treatment by rifampicin drastically decreased [^{11}C]glyburide uptake by the liver (Fig. 2) with a 48.5 ± 6.5 % decrease in liver exposure (AUC_{liver}, Fig. 3 and Table 1). Consistently, kinetic modeling confirmed a 77.3 ± 7.3 % decrease in the transfer constant of [^{11}C]glyburide from blood to the liver (k_{uptake}) which ranged from − 67.4 % to − 87.9 % among subjects (Fig. 4). The magnitude of the decrease in k_{uptake} in response to inhibition was strongly correlated with baseline k_{uptake} (Fig. 4C, R^2 = 0.98, p < 0.01).

As a consequence to decreased liver uptake, OATP inhibition using rifampicin significantly increased concentrations of [^{11}C]glyburide in the vasculature (Figs. 2 and 3 and Table 1). AUC_{blood} was significantly higher (p = 0.003, n = 5) after treatment with rifampicin (mean increase of + 25.0 ± 10.3 %, n = 5) (Table 1). Urinary bladder was more obvious on PET images after rifampicin infusion (Fig. 2). Urinary clearance of radioactivity was not significantly modified at 30 min after treatment by rifampicin (Supplemental Fig. 2A). Radioactivity detected in urine almost exclusively corresponded to radiometabolites (n = 10 samples in both baseline and rifampicin-treated conditions) (Supplemental Fig. 2B).

Pretreatment by rifampicin increased tissue exposure ($AUC_{0–30\ min}$) for kidneys (+ 21.5 ± 12.1, p = 0.0043) and myocardium (+ 43.3 ± 25.1, p = 0.034) (Table 1). Transfer constants from blood to the tissues (k_{uptake}) could not be accurately estimated in organs other than the liver. Importance of OATP function for distribution of [^{11}C]glyburide to tissues was therefore estimated as change in AUCR. No significant change in AUCR could be observed in organs other than the liver suggesting limited importance of OATP in mediating the tissue distribution of [^{11}C]glyburide in other tissues (Table 1).

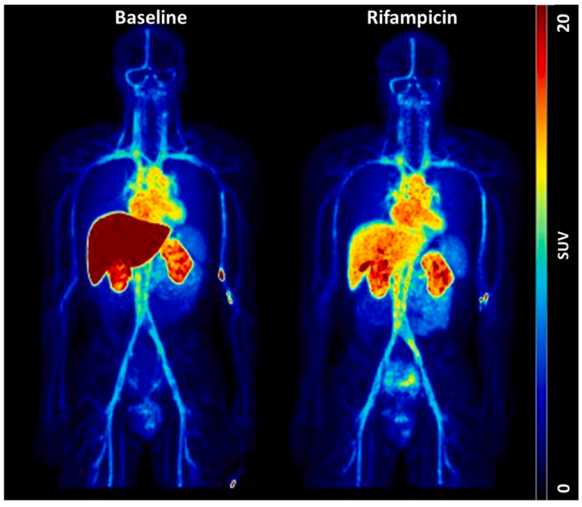

Fig. 2. Whole-body PET images of [^{11}C] glyburide distribution in baseline condition and after treatment with rifampicin (9 mg/kg i.v.) in a healthy volunteer. Images are the maximum intensity projections of the frames summed from 3 to 30 min and are expressed in standardized uptake values (SUV).

4. Discussion

DWB-PET imaging using [^{11}C]glyburide was performed in humans to investigate the WBPK of glyburide and estimate the importance of OATP function on drug delivery to tissues. The main result of the study was the dramatic impact of OATP inhibition using rifampicin on the liver uptake of [^{11}C]glyburide in humans. Rifampicin decreased the liver AUCR by 58.7 ± 5.2 % and the k_{uptake} by 77.3 ± 7.3 %, suggesting high importance of OATP in controlling the uptake of glyburide by human hepatocytes. A preclinical study using [^{11}C]glyburide PET in non-human primates demonstrated that the OATP inhibitors rifampicin (same dose than in the present study) or cyclosporin (15 mg/kg/h, i.v.) decreased the liver uptake of [^{11}C]glyburide in a higher extent (− 90 % in $AUCR_{liver}$) [36]. This is consistent with the higher expression of OATP1B1, assessed using quantitative proteomics, in the liver of non-human primates compared with humans, suggesting species differences in liver OATP function [37].

Our clinical data show that [^{11}C]glyburide is poorly metabolized in humans, which is consistent with the known PK of glyburide (< 5 % proportion of 4-hydroxy-glyburide in plasma over 24 h) [28]. This is a major advantage because it enables correct interpretation of PET data, assuming suitable radiochemical purity of the PET signal in tissues over the investigated timeframe. Metabolic stability of [^{11}C]glyburide is a major asset compared with previous OATP probes which are extensively metabolized. Radiometabolites of [^{11}C]dehydropravastatin were predominant in human blood at 30 min [22]. (15 *R*)-[^{11}C]TIC-Me is a prodrug that is rapidly metabolized into (15*R*)-[^{11}C]TIC (10 min) which is the OATP substrate, and for which another radiometabolite becomes predominant after 20 min [22,24].

Liver uptake of [^{11}C]glyburide in humans was very sensitive to the inhibition by rifampicin as revealed by the ~ 77% decrease in k_{uptake}. In comparison, only 25 % decrease in the uptake of [^{11}C]erlotinib was observed after treatment by rifampicin (600 mg i.v.), 45 % for (15*R*)-

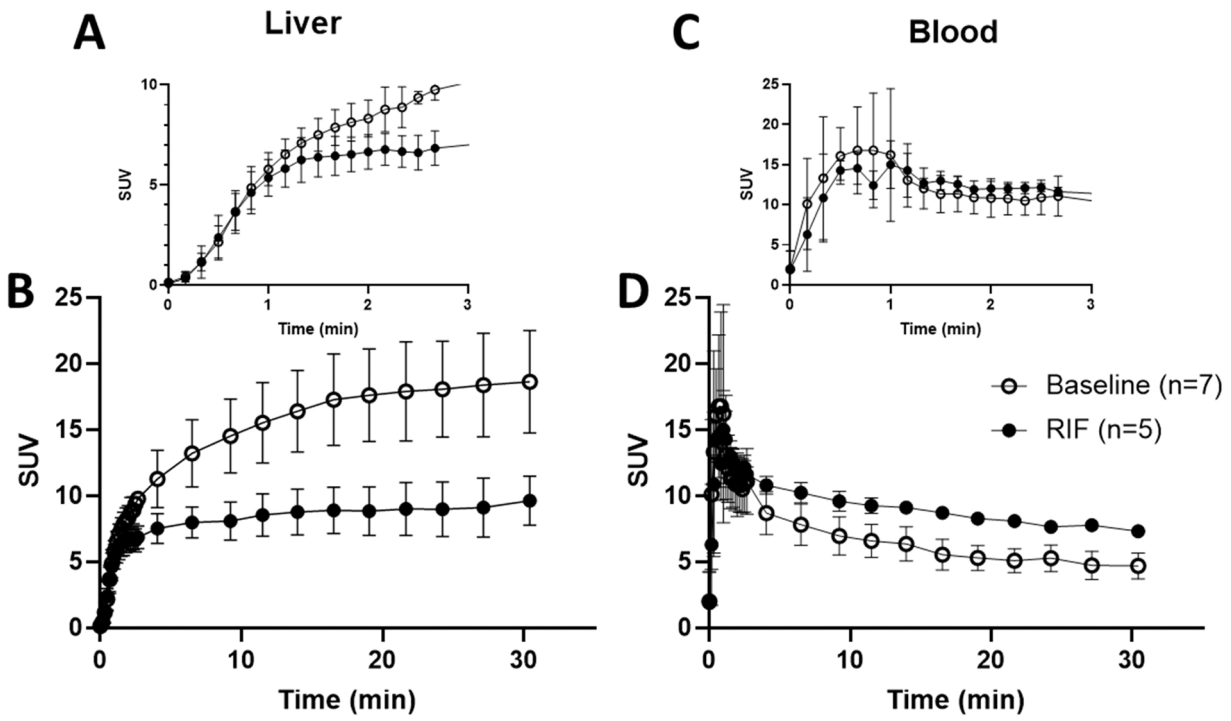

Fig. 3. Time-activity curves of [^{11}C]glyburide in liver (A, B) and blood (image-derived, C, D) in baseline conditions and after treatment with rifampicin (9 mg/kg i.v.) from 0 to 30 min (B, D) and with a focus from 0 to 3 min (A, C). Data are mean ± SD.

Table 1
Areas under the curve (AUC) and area under the curve ratios (AUCR = AUC_{tissue}/AUC_{blood}) of the time-activity curves of [^{11}C] glyburide calculated for each subject in baseline condition and after treatment with rifampicin (9 mg/kg i.v.). Reported blood pool data come from the validated image-derived input function. Data are mean ± SD; *, $p < 0.05$, paired t-test compared to baseline).

	AUC (SUV.min)		AUCR (AUC_{tissue}/AUC_{blood})	
	Baseline	Rifampicin	Baseline	Rifampicin
Blood pool	208.15 ± 23.91	258.20 ± 10.73*	–	–
Liver	444.66 ± 52.22	228.79 ± 36.59*	2.17 ± 0.45	0.89 ± 0.16*
Kidneys	207.31 ± 17.00	250.92 ± 21.58*	1.00 ± 0.10	0.95 ± 0.11
Spleen	102.70 ± 7.22	119.35 ± 14.24*	0.50 ± 0.07	0.46 ± 0.07
Myocardium	94.85 ± 19.35	132.15 ± 6.25*	0.46 ± 0.07	0.51 ± 0.02
Pancreas	164.86 ± 30.64	178.48 ± 32.05	0.79 ± 0.11	0.69 ± 0.12
Brain	5.82 ± 0.74	7.72 ± 0.69*	0.03 ± 0.00	0.03 ± 0.00
Testis	56.12 ± 22.17	67.30 ± 23.27	0.22 ± 0.06	0.26 ± 0.10
Muscle	9.69 ± 3.83	10.66 ± 0.80	0.04 ± 0.01	0.04 ± 0.00
Eyes	2.34 ± 0.38	4.60 ± 4.18	0.01 ± 0.00	0.02 ± 0.02

[^{11}C]TIC and 58 % for [^{11}C]dehydropravastatin (both using the same dose of rifampicin 600 mg *per os*) [20,22,24]. High response to OATP inhibition by rifampicin compared to previous radioligands suggests exquisite sensitivity of [^{11}C]glyburide to detect change in transporter function, in a limited number of subjects. [^{11}C]glyburide is a poorly permeable, highly lipophilic compound, with high binding to plasma proteins. It may be hypothesized that transport of [^{11}C]glyburide across the basolateral pole of hepatocytes may be predominantly governed by OATP function, with negligible concurrent passive diffusion. Consistently, k_{uptake} of [^{11}C]glyburide during OATP inhibition was extremely low (0.0154 ± 0.074 min^{-1}) suggesting that almost complete OATP inhibition was achieved, leading to low uptake by hepatocytes. Li et al. used *in vitro* models to simulate the liver uptake clearance of glyburide and concluded that OATP-mediated uptake accounted for 98% of the total liver uptake of glyburide (5560 L/h for carrier-mediated transport *vs* 111 L/h for passive diffusion) [26]. They also suggested that liver uptake of metabolites is ~ 10-fold lower compared with parent glyburide, thus supporting suitable radiochemical purity of the PET signal for [^{11}C]glyburide in the liver [26]. A large and consistent body of research suggests that the liver uptake of glyburide is predominantly mediated by OATP transporter(s) [26,38,39]. However, contribution of other transporters in the liver uptake of [^{11}C]glyburide cannot be excluded. To the best of our knowledge, glyburide has not been reported as a substrate of organic cation transporter 1 (OCT1), another important influx transporter expressed at the sinusoidal pole of hepatocytes [38,39]. In our study, almost complete inhibition of the liver uptake of [^{11}C]glyburide was achieved using rifampicin which may inhibit multiple hepatocyte transporters including OATPs but does not inhibit OCT1 [40,41]. Therefore, comparison of the transporter substrate/inhibitor profile of glyburide and rifampicin does not support a role for OCT1 in controlling the liver uptake of glyburide in humans.

Altogether, our PET data interpreted in the light of previous *in vitro* data, suggest that the uptake of [^{11}C]glyburide by the liver is predominantly governed by OATPs. Compared with previously reported OATP probes, [^{11}C]glyburide benefits from exquisite sensitivity and suitable radiochemical purity of the PET signal in both the blood and the liver. The negligible proportion of radiometabolites in the blood and liver allows for correct estimation of the OATP-mediated transport capacity of hepatocytes which was a major limitation of previous PET radioligands that undergo substantial liver metabolism [14,19].

The magnitude of response to inhibition, which requires two subsequent PET scans prior to and after OATP inhibition, was used to estimate the total transport capacity of OATP in the liver. Interestingly, baseline k_{uptake} accurately predicted the magnitude of response to inhibition.

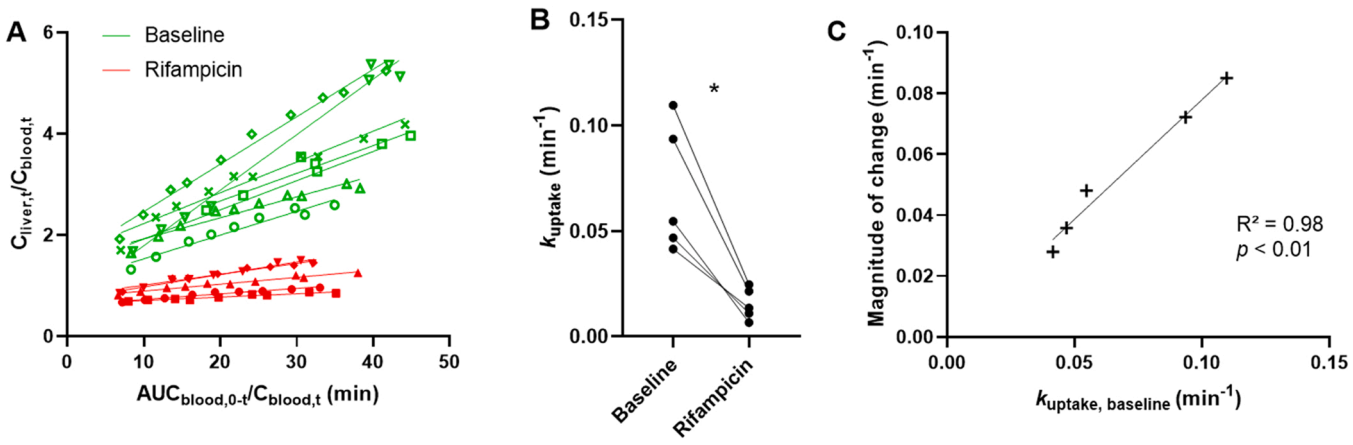

Fig. 4. Transfer of [^{11}C] glyburide from blood to the liver assessed by integration plot analysis from 5 to 30 min (A), change in transfer constant (k_{uptake}) (B), and magnitude of the decrease in k_{uptake} (C) for each subject between baseline condition and after treatment with rifampicin (9 mg/kg i.v.). Blood data come from a validated image-derived input function. The k_{uptake} was assessed from the integration plot analysis by determining the slope of the regression plot for each PET acquisition (*, $p < 0.05$, paired *t*-test). The magnitude of change was assessed by subtracting for each subject k_{uptake} after treatment by rifampicin to k_{uptake} in baseline condition.

Two subsequent scans will still be needed to investigate the risk of DDIs involving OATPs using [^{11}C]glyburide, as exemplified with rifampicin in the present study. However, our results suggest that a single [^{11}C]glyburide PET scan is sufficient for quantitative determination of the total transport capacity of OATP, given the limited importance of non-OATP-mediated uptake of [^{11}C]glyburide by the liver. This allows for quantitative study of the regulation of OATP activity observed in various patho-physiological situations [42]. Imaging liver OATP function using [^{11}C]glyburide PET may therefore be useful as a molecular determinant of liver function in animal model or patients with liver dysfunction. To the best of our knowledge, such property has not been demonstrated for previous PET probes for OATPs.

The WBPK approach used in this study illustrates the relevance of DWB-PET imaging to explore the impact of transporter-mediated DDI at both the blood and the tissue levels [13]. Interestingly, the DDI between glyburide and rifampicin was initially described through the magnitude change in plasma concentration of glyburide in a clinical PK study [28]. In a population similar to ours, a same i.v. infusion dose of rifampicin (600 mg) significantly increased the plasma AUC of orally administered glyburide by 125 ± 51.5 % compared with the baseline situation. Magnitude of this DDI was much higher than the change observed in our study (25.0 ± 10.3 %) [28] which may be explained by several methodological differences. First, glyburide was given orally at a dose of 1.25 mg while in our study [^{11}C]glyburide was given i.v. at microdoses (11.2 ± 5.8 μg). Above all, our PET data were obtained only the 30 min after injection, thus predominantly reflecting the distribution phase while the plasma PK study reported by Zheng et al. was carried out over 24 h, mainly reflecting the elimination phase. This suggests that early PET data may underestimate the overall impact of transporter-mediated DDI on drug elimination, especially when hepatic elimination is involved [28]. Altogether, this suggests that WBPK imaging using short-life isotopes such as carbon-11 is useful to unveil the tissue distribution of drugs but may not accurately capture the entirety of the plasma PK of drugs with longer plasma half-life. PK PET data should be interpreted in the light of known plasma PK but cannot not replace it.

The DWB-PET protocol enabled direct visualization of the WBPK of glyburide. Our results show that dramatic decrease in liver uptake of [^{11}C]glyburide resulted in increased exposure in the blood and several organs including kidneys, myocardium, spleen, and brain. Increase in the pancreas, which is assumed to be the target tissue for glyburide, was not significant ($p > 0.05$). This may be due to poor quantification associated with low uptake and radioactive counting compared with surrounding abdominal tissues. From a therapeutic perspective, this suggests that modest uptake suffices to promote insulin release by pancreatic cells, although extra-pancreatic mechanism of action has been proposed for glyburide, with a central role of the liver [43]. From an imaging perspective, this suggests that [^{11}C]glyburide is not appropriate as a probe for imaging SUR1 expression in the pancreas.

In non-human primates, rifampicin-inhibitable uptake of [^{11}C]glyburide occurred in the myocardium and kidney cortex suggesting a functional role for non-hepatic OATPs in these organs [36]. This was not observed in humans suggesting a limited role for non-hepatic OATPs in controlling the blood-to-tissue uptake of [^{11}C]glyburide [44]. Non-hepatic OATPs of putative importance for PK are OATP2B1 and OATP1A2 which are ubiquitously expressed [7]. However, non-hepatic tissues with reported OATP2B1, OATP1A2 or OATP1B3 expressions such as the brain, kidneys, myocardium, spleen, pancreas, testis, muscle, and eyes display very low baseline uptake of [^{11}C]glyburide and no or limited changes in AUCR after OATP inhibition using rifampicin [8]. Altogether, this suggests that in human [^{11}C]glyburide behaves as a liver-specific OATP substrate *in vivo*, suggesting species differences in the importance of non-hepatic OATPs [45].

Several hypotheses can be drawn to explain this result with respect to investigated organs. First, recent *in vitro* and simulation studies, performed using MDCKII-cells transfected with the human genes, suggest that glyburide may specifically be transported by OATP1B1 which is a liver-specific member. In the brain, PET images showed the negligible uptake of [^{11}C]glyburide although OATP2B1 and OATP1A2 are expressed at the BBB (Fig. 2) [8,46]. [^{11}C]glyburide is transported by efflux transporters from the ATP-Binding Cassette (ABC) family such as the P-glycoprotein (P-gp, ABCB1) and the breast cancer resistance protein (BCRP, ABCG2) which restrict the brain penetration of their substrates across the BBB [47–50,36,51]. In this situation, a competition may occur between influx and efflux transporters at the same interface [14]. The role of OATPs expressed in the kidneys such as OATP4C1 is poorly understood [52]. Given the high proportion of radiometabolites in urine, the radio-HPLC analysis of urine samples was not sensitive enough to detect the excreted amount of parent (unmetabolized) [^{11}C] glyburide at the end of PET acquisition. It was therefore not possible to assess whether rifampicin altered CL_{urine} of [^{11}C]glyburide from our PET data. In a clinical PK study, Zheng et al. consistently showed that the 0–12 h accumulated amount of glyburide in urine was 198-fold lower than that of metabolite (4-hydroxyglyburide) in baseline condition, and 117-fold after OATP inhibition using i.v rifampicin [28]. Moreover, they reported no change in the urinary clearance of glyburide and 4-hydroxy-glyburide after rifampicin injection, suggesting a limited role for

rifampicin-inhibitable transport in controlling the urinary clearance of glyburide in humans [28]. Additionally, *in vitro* studies suggest that the metabolites of glyburide, but not glyburide itself, are secreted in the urine *via* the organic anion transporters 3 (OAT3) expressed on the basolateral membrane of the kidney proximal tubule cells [26]. Further experiments are needed to untangle the importance of carrier-mediated processes, which may involve influx and efflux transporters, for the renal elimination of glyburide and its metabolites.

To the best of our knowledge, it is the first application of PET-MR DWB imaging for the study of dynamic processes such as PK and DDIs in humans. Compared with current static or whole-body acquisition routinely performed using PET-CT (computed tomography) scanners, DWB imaging PET-MR reduces volunteer exposure to radiation, allows for repeated scanning without additional CT for attenuation correction, and ensures accurate delineation in organs including soft tissues [53]. This original method enables quantification of radiolabeled substrates of transporters in several organs in a parallel manner which in turn allows for direct comparison of the importance of transporter function between organs in each individual. This suggests that the development of DWB acquisition and total-body scanners may foster the use of PET imaging to elucidate the WBPK in early drug development as part of clinical pharmacology studies [54]. Finally, efforts are being made to ensure suitable drug delivery to tissues while reducing liver exposure of drugs and/or metabolites and prevent drug-induced liver injury (DILI) [55,56]. Our clinical results suggest that almost complete inhibition of liver OATP function can be achieved using a clinical dose of rifampicin. Given the limited role for non-hepatic OATPs in controlling the uptake of drugs by tissues, this strategy may be further used to block the liver uptake of OATP substrates while ensuring increased delivery to other organs, which can be monitored using DWB-PET.

5. Conclusion

[^{11}C]glyburide was validated as a PET probe for imaging OATP function in the human liver. [^{11}C]glyburide benefits from suitable PK properties including metabolic stability and high magnitude of response to OATP inhibition, suggesting suitable sensitivity and specificity. [^{11}C] glyburide provides a relevant tool to investigate OATP-mediated DDI at the liver level or the regulation of OATP function in health and disease. The use of a WBD PET-MR acquisition provided unique information on the impact of OATP-mediated DDIs on tissue exposure to drugs which brings new insights for WBPK and carrier-mediated drug delivery to the whole-body in humans.

CRediT authorship contribution statement

TOURNIER Nicolas contributed to the study conception and design. Material preparation, data collection and analysis were performed by MARIE Solène, CHALAMPALAKIS Zacharias, BREUIL Louise, BECQUEMONT Laurent, LECOQ Anne-Lise, CAILLÉ Fabien, GERVAIS Philippe, COMTAT Claude, BOTTLAENDER Michel, and TOURNIER Nicolas. The first draft of the manuscript was written by MARIE Solène and all authors commented on previous versions of the manuscript. All authors read and approved the final manuscript.

Data Availability

The datasets generated during and/or analyzed during the current study are available from the corresponding author on reasonable request.

Funding

This work was funded by Grant ANR-16-CE17-0011 and performed on a platform member of France Life Imaging Network (Grant ANR-11-INBS-0006). Zacharias CHALAMPALAKIS and Claude COMTAT received funding for this project from the European Union's Horizon 2020 research and innovation program under the Marie Sklodowska-Curie Grant agreement no. 764458.

Ethics approval

This study was performed in line with the principles of the Declaration of Helsinki. Approval was granted by the Ethics Committee (CPP IDF 5: 17041).

Consent to participate

Signed informed consent was obtained from all individual participants included in the study.

Consent to publish

The authors affirm that human research participants provided informed consent for publication of the images in Fig. 2.

Clinical Trial Registration

EudraCT 2017-001703-69 registered the 21 September 2017.

Conflict of interest statement

The authors declare that there are no conflicts of interest.

Data Availability

Data will be made available on request.

Acknowledgments

The authors thank Maud GOISLARD, Christine BARON, and Thierry LEKIEFFRE for technical assistance.

Appendix A. Supporting information

Supplementary data associated with this article can be found in the online version at doi:10.1016/j.biopha.2022.113994.

References

[1] S. McFeely, L. Wu, T. Ritchie, J. Unadkat, Organic anion transporting polypeptide 2B1 – More than a glass-full of drug interactions, Pharm. Ther. 196 (2019) 204–215.
[2] S.K. Nigam, What do drug transporters really do? Nat. Rev. Drug Discov. 14 (2015) 29–44.
[3] K.M. Giacomini, S.-M. Huang, D.J. Tweedie, L.Z. Benet, K.L.R. Brouwer, X. Chu, et al., Membrane transporters in drug development, Nat. Rev. Drug Discov. 9 (2010) 215–236.
[4] H. Kusuhara, Y. Sugiyama, Role of transporters in the tissue-selective distribution and elimination of drugs: transporters in the liver, small intestine, brain and kidney, J. Control. Release 78 (2002) 43–54.
[5] D. Kovacsics, I. Patik, C. Özvegy-Laczka, The role of organic anion transporting polypeptides in drug absorption, distribution, excretion and drug-drug interactions, Expert Opin. Drug Metab. Toxicol. 0 (2016) 1–16.
[6] M. Kim, P. Deacon, R. Tirona, R. Kim, C. Pin, H. Meyer zu Schwabedissen, et al., Characterization of OATP1B3 and OATP2B1 transporter expression in the islet of the adult human pancreas, Histochem Cell Biol. 148 (2017) 345–357.
[7] M. Roth, A. Obaidat, B. Hagenbuch, OATPs, OATs and OCTs: the organic anion and cation transporters of the SLCO and SLC22A gene superfamilies, Br. J. Pharm. 165 (2012) 1260.
[8] B. Hagenbuch, B. Stieger, The SLCO (former SLC21) superfamily of transporters, Mol. Asp. Med. 34 (2013) 396.
[9] S. Li, Y. Yu, Z. Jin, Y. Dai, H. Lin, Z. Jiao, et al., Prediction of pharmacokinetic drug-drug interactions causing atorvastatin-induced rhabdomyolysis using physiologically based pharmacokinetic modelling, Biomed. Pharmacother. Biomed. Pharmacother. 119 (2019), 109416.
[10] I. Nestorov, Whole body pharmacokinetic models, Clin. Pharmacokinet. 42 (2003) 883–908.

[11] M. Rizk, L. Zou, R. Savic, K. Dooley, Importance of drug pharmacokinetics at the site of action, Clin. Transl. Sci. 10 (2017) 133–142.
[12] T. Burt, G. Young, W. Lee, H. Kusuhara, O. Langer, M. Rowland, et al., Phase 0/microdosing approaches: time for mainstream application in drug development? Nat. Rev. Drug Discov. 19 (2020) 801–818.
[13] A. Rahmim, M.A. Lodge, N.A. Karakatsanis, V.Y. Panin, Y. Zhou, A. McMillan, et al., Dynamic whole-body PET imaging: principles, potentials and applications, Eur. J. Nucl. Med. Mol. Imaging 46 (2019) 501–518.
[14] N. Tournier, B. Stieger, O. Langer, Imaging techniques to study drug transporter function in vivo, Pharm. Ther. 189 (2018) 104–122.
[15] W.M. Arif, P.H. Elsinga, C. Gasca-Salas, M. Versluis, R. Martínez-Fernández, R.A.J. O. Dierckx, et al., Focused ultrasound for opening blood-brain barrier and drug delivery monitored with positron emission tomography, J. Control. Release 324 (2020) 303–316.
[16] L. Garcia-Varela, P. Mossel, P. Aguiar, D.A. Vazquez-Matias, A. van Waarde, A.T. M. Willemsen, et al., Dose-response assessment of cerebral P-glycoprotein inhibition in vivo with [18F]MC225 and PET, J. Control. Release 347 (2022) 500–507.
[17] S. Mairinger, I. Hernández-Lozano, T. Filip, M. Sauberer, M. Löbsch, J. Stanek, et al., Impact of P-gp and BCRP on pulmonary drug disposition assessed by PET imaging in rats, J. Control. Release 349 (2022) 109–117.
[18] T. Sugiura, Y. Kato, A. Tsuji, Role of SLC xenobiotic transporters and their regulatory mechanisms PDZ proteins in drug delivery and disposition, J. Control. Release 116 (2006) 238–246.
[19] S. Marie, S. Cisternino, I. Buvat, X. Declèves, N. Tournier, Imaging probes and modalities for the study of solute carrier O (SLCO)-transport function in vivo, J. Pharm. Sci. 106 (2017) 2335–2344.
[20] M. Bauer, A. Matsuda, B. Wulkersdorfer, C. Philippe, A. Traxl, C. Özvegy-Laczka, et al., Influence of OATPs on hepatic disposition of erlotinib measured with positron emission tomography, Clin. Pharm. Ther. 104 (2018) 139–147.
[21] S. Billington, S. Shoner, S. Lee, K. Clark-Snustad, M. Pennington, D. Lewis, et al., PET imaging of [11C]Rosuvastatin hepatic concentrations and hepatobiliary transport in humans in the absence and presence of cyclosporine A, Clin. Pharm. Ther. 106 (2019) 1056–1066.
[22] K. Kaneko, M. Tanaka, A. Ishii, Y. Katayama, T. Nakaoka, S. Irie, et al., A clinical quantitative evaluation of hepatobiliary transport of [11C]Dehydropravastatin in humans using positron emission tomography, Drug Metab. Dispos. 46 (2018) 719–728.
[23] K. Maeda, A. Ohnishi, M. Sasaki, Y. Ikari, K. Aita, Y. Watanabe, et al., Quantitative investigation of hepatobiliary transport of [11C]telmisartan in humans by PET imaging, Drug Metab. Pharmacokinet. 34 (2019) 293–299.
[24] T. Takashima, S. Kitamura, Y. Wada, M. Tanaka, Y. Shigihara, H. Ishii, et al., PET imaging–based evaluation of hepatobiliary transport in humans with (15R)-11C-TIC-Me, J. Nucl. Med. 53 (2012) 741–748.
[25] L. Mack, P. Tomich, Gestational diabetes: diagnosis, classification, and clinical care, Obstet. Gynecol. Clin. N. Am. 44 (2017) 207–217.
[26] R. Li, Y. Bi, A. Vildhede, R.J. Scialis, S. Mathialagan, X. Yang, et al., Transporter-mediated disposition, clinical pharmacokinetics and cholestatic potential of glyburide and its primary active metabolites, Drug Metab. Dispos. Am. Soc. Pharmacol. Exp. Ther. 45 (2017) 737–747.
[27] S. Vavricka, J. Van Montfoort, H. Ha, P. Meier, K. Fattinger, Interactions of rifamycin SV and rifampicin with organic anion uptake systems of human liver, Hepatology 36 (2002) 164–172.
[28] H. Zheng, Y. Huang, L. Frassetto, L. Benet, Elucidating Rifampin's inducing and inhibiting effects on glyburide pharmacokinetics and blood glucose in healthy volunteers: unmasking the differential effect of enzyme induction and transporter inhibition for a drug and its primary metabolite, Clin. Pharm. Ther. 85 (2009) 78.
[29] A. Koenen, K. Köck, M. Keiser, W. Siegmund, H. Kroemer, M. Grube, Steroid hormones specifically modify the activity of organic anion transporting polypeptides, Eur. J. Pharmaceut. Sci. 47 (2012) 774–780.
[30] H. Satoh, F. Yamashita, M. Tsujimoto, H. Murakami, N. Koyabu, H. Ohtani, et al., Citrus juices inhibit the function of human organic anion-transporting polypeptide Oatp-B, Drug Metab. Dispos. 33 (2005) 518–523.
[31] F. Caillé, P. Gervais, S. Auvity, C. Coulon, S. Marie, N. Tournier, et al., Automated two-step manufacturing of [11C]glyburide radiopharmaceutical for PET imaging in humans, Nucl. Med. Biol. 84–85 (2020) 20–27.
[32] H.J. Rogers, R.G. Spector, P.J. Morrison, I.D. Bradbrook, Pharmacokinetics of intravenous glibenclamide investigated by a high performance liquid chromatographic assay, Diabetologia 23 (1982) 37–40.
[33] D. Amor, S. Goutal, S. Marie, F F, M. Bauer, O. Langer, et al., Impact of rifampicin-inhibitable transport on the liver distribution and tissue kinetics of erlotinib assessed with PET imaging in rats, EJNMMI Res. 8 (2018) 81.
[34] N. Tournier, S. Cisternino, M. Peyronneau, S. Goutal, F. Dolle, J. Scherrmann, et al., Discrepancies in the P-glycoprotein-mediated transport of (18)F-MPPF: a pharmacokinetic study in mice and non-human primates, Pharmaceut. Res. 29 (2012) 2468–2476.
[35] K.M. Olsen, G.L. Kearns, S.F. Kemp, Glyburide protein binding and the effect of albumin glycation in children, young adults, and older adults with diabetes, J. Clin. Pharm. 35 (1995) 739–745.
[36] N. Tournier, W. Saba, S. Cisternino, M. Peyronneau, A. Damont, S. Goutal, et al., Effects of selected OATP and/or ABC transporter inhibitors on the brain and whole-body distribution of glyburide, AAPSJ. 15 (2013) 1082–1090.
[37] L. Wang, B. Prasad, L. Salphati, X. Chu, A. Gupta, C. Hop, et al., Interspecies variability in expression of hepatobiliary transporters across human, dog, monkey, and rat as determined by quantitative proteomics, Drug Metab. Dispos. 43 (2015) 367–374.
[38] S. Klatt, M.F. Fromm, J. König, Transporter-mediated drug-drug interactions with oral antidiabetic drugs, Pharmaceutics 3 (2011) 680–705.
[39] S. Marie, K.L. Frost, R.K. Hau, L. Martinez-Guerrero, J.M. Izu, C.M. Myers, et al., Predicting disruptions to drug pharmacokinetics and the risk of adverse drug reactions in non-alcoholic steatohepatitis patients, Acta Pharm. Sin. B [Internet], 2022 [cited 2022 Nov 7]; Available from: ⟨https://www.sciencedirect.com/science/article/pii/S2211383522003690⟩).
[40] M.M. Parvez, N. Kaisar, H.J. Shin, J.A. Jung, J.-G. Shin, Inhibitory interaction potential of 22 antituberculosis drugs on organic anion and cation transporters of the SLC22A family, Antimicrob. Agents Chemother. 60 (2016) 6558–6567.
[41] M.M. Parvez, J.A. Jung, H.J. Shin, D.H. Kim, J.-G. Shin, Characterization of 22 antituberculosis drugs for inhibitory interaction potential on organic anionic transporter polypeptide (OATP)-mediated uptake, Antimicrob. Agents Chemother. 60 (2016) 3096–3105.
[42] M. Droździk, S. Oswald, A. Droździk, Impact of kidney dysfunction on hepatic and intestinal drug transporters, Biomed. Pharmacother. Biomed. Pharmacother. 143 (2021), 112125.
[43] L. Luzi, G. Pozza, Glibenclamide: an old drug with a novel mechanism of action? Acta Diabetol. 34 (1997) 239–244.
[44] J. Kinzi, M. Grube, H. Meyer zu Schwabedissen, OATP2B1 – the underrated member of the organic anion transporting polypeptide family of drug transporters? Biochem. Pharm. 188 (2021), 114534.
[45] T. Takahashi, Y. Uno, H. Yamazaki, T. Kume, Functional characterization for polymorphic organic anion transporting polypeptides (OATP/SLCO1B1, 1B3, 2B1) of monkeys recombinantly expressed with various OATP probes, Biopharm. Drug Dispos. 40 (2019) 62–69.
[46] S. Marie, C. Comtat, F. Caillé, L. Becquemont, M. Bottlaender, N. Tournier, ^{11}C-glyburide PET imaging unveils the negligible brain penetration of glyburide in humans, Neurology 92 (2019) 813–814.
[47] L. Cygalova, J. Hofman, M. Ceckova, F. Staud, Transplacental pharmacokinetics of glyburide, rhodamine 123, and BODIPY FL prazosin: effect of drug efflux transporters and lipid solubility, J. Pharm. Exp. Ther. 331 (2009) 1118–1125.
[48] C. Gedeon, J. Behravan, G. Koren, M. Piquette-Miller, Transport of glyburide by placental ABC transporters: implications in fetal drug exposure, Placenta 27 (2006) 1096–1102.
[49] S. Hemauer, S. Patrikeeva, T. Nanovskaya, G. Hankins, M. Ahmed, Role of human placental apical membrane transporters in the efflux of glyburide, rosiglitazone, and metformin, Am. J. Obstet. Gynecol. 202 (2010) 383.e1–383.e7.
[50] E. Pollex, A. Lubetsky, G. Koren, The role of placental breast cancer resistance protein in the efflux of glyburide across the human placenta, Placenta 29 (2008) 743–747.
[51] L. Zhou, S. Naraharisetti, H. Wang, J. Unadkat, M. Hebert, Q. Mao, The breast cancer resistance protein (Bcrp1/Abcg2) limits fetal distribution of glyburide in the pregnant mouse: an obstetric-fetal pharmacology research unit network and university of Washington Specialized Center of research study, Mol. Pharm. 73 (2008) 949–959.
[52] W. Zou, B. Shi, T. Zeng, Y. Zhang, B. Huang, B. Ouyang, et al., Drug transporters in the kidney: perspectives on species differences, disease status, and molecular docking, Front. Pharm. 12 (2021), 746208.
[53] N. Tournier, C. Comtat, V. Lebon, J.-L. Gennisson, Challenges and perspectives of the hybridization of PET with functional MRI or ultrasound for neuroimaging, Neuroscience (2020).
[54] S.R. Cherry, T. Jones, J.S. Karp, J. Qi, W.W. Moses, R.D. Badawi, Total-body PET: maximizing sensitivity to create new opportunities for clinical research and patient care, J. Nucl. Med. 59 (2018) 3–12.
[55] G. Pan, Roles of hepatic drug transporters in drug disposition and liver toxicity, Adv. Exp. Med. Biol. 1141 (2019) 293–340.
[56] A. Ghallab, R. Hassan, U. Hofmann, A. Friebel, Z. Hobloss, L. Brackhagen, et al., Interruption of bile acid uptake by hepatocytes after acetaminophen overdose ameliorates hepatotoxicity, J. Hepatol. 77 (2022) 71–83.